



Sea buckthorn pulp oil nanoemulsions fabricated by ultra-high pressure homogenization process: A promising carrier for nutraceutical

Ming Chang^a, Yiwen Guo^a, Zhongrong Jiang^c, Longkai Shi^a, Tao Zhang^a, Yandan Wang^a, Mengyue Gong^a, Tao Wang^a, Ruixue Lin^a, Ruijie Liu^{a,*}, Yong Wang^b, Qingzhe Jin^a, Xingguo Wang^a

^a State Key Laboratory of Food Science and Technology, Synergetic Innovation Center of Food Safety and Nutrition, School of Food Science and Technology, Jiangnan University, Wuxi, 214000, China

^b Guangdong Saskatchewan Oilseed Joint Laboratory, Department of Food Science and Engineering, Science and Engineering Jinan University, Guangzhou, 510632, China

^c Technology Center, China Tobacco Sichuan Industrial Co., Ltd., Chengdu, 610066, China

ARTICLE INFO

Keywords:

Sea buckthorn pulp oil
Ultra-high pressure homogenization
Nanoemulsions
Sodium caseinate
Stability
Antioxidant activity

ABSTRACT

Food protein-stabilized with nanoemulsions were prepared by ultra-high pressure homogenization under appropriate homogenization condition, so as to improve the poor water solubility and instability of sea buckthorn pulp oil (SBPO). SBPO nanoemulsions stabilized by sodium caseinate (SC) and whey protein isolates (WPI) suggested good microstructures and rheological properties. SC-stabilized SBPO nanoemulsions system showed smaller mean particle size (<260 nm), lower K_e value (6.3–20.4%) and higher absolute value of zeta potential (55.70–67.20mV) over various pH (3–9), salinity (0–200 mM), temperature (20–80 °C). The SC-stabilized SBPO nanoemulsions showed no significantly increase in droplet size over 30 days at 4 °C and 25 °C, which proved it has good stability. The antioxidant activity of SC-stabilized SBPO nanoemulsions was evaluated by employing cellular antioxidant activity (CAA) model and the results showed good antioxidant activity. This study implied that protein-stabilized nanoemulsions are a promising carrier for extending the applications of SBPO as nutraceutical or functional dairy beverage.

1. Introduction

Sea buckthorn pulp oil (SBPO), a nutritive oil product obtained from the pulp of the SB berry, has been received attention in recent years for its healthy properties (Gao et al., 2017). SBPO is characterized by an abundant composition of fatty acids, chemically includes palmitoleic acid (C16:1, 19.4%~38.5%), palmitic acid (C16:0, 28.9%~37.8%), oleic acid (C18:1, 10.8%~33.6%), linoleic acid (C18:2, 4.1%~14.2%) and α -linolenic acid (C18:3, 1.6%~7.4%) (Zheng et al., 2017), which may be related to the fruit maturity, storage time, planting conditions (Fatima et al., 2012; George and Cenkowski, 2007). In addition, SBPO is one of the most special edible oils because of its enrichment lipids phytochemical, including tocopherols, phytosterols and carotenoids (Fatima et al., 2012). Currently, SB has been applied in the cosmetic and health products industries, including chewable tablets and sunscreen cream (Zielińska and Nowak, 2017). Despite the advantages of SBPO,

the poor water solubility and phytochemical instability limits the application of SBPO in food fields.

Nanoemulsions are emerging as a good alternative to deliver and protect lipophilic functional substances, because they have many advantages compared with traditional emulsions. The principal advantages of nanoemulsions are easy to prepare, improved the stability of system, enhance delivery substances solubility and bioavailability (Joye et al., 2014; Rave et al., 2020). However, nanoemulsions are non-equilibrium system that may produce flocculation. The electrostatic repulsion and space stabilizing force generated by the adsorption layer of the emulsifier can prevent the flocculation of the droplets (Xu et al., 2017). Food-grade proteins generally show good stability and suppressed coalescence in the preparation of nanoemulsions for hydrophobic functional components. These proteins include sodium caseinate (SC), whey protein isolates (WPI), and soybean proteins isolate (SPI) (Singh and Sarkar, 2011). These proteins have good amphiphilic and

* Corresponding author.

E-mail address: ruijieliu-2007@hotmail.com (R. Liu).

<https://doi.org/10.1016/j.jfoodeng.2020.110129>

Received 27 January 2020; Received in revised form 6 May 2020; Accepted 7 May 2020

Available online 10 May 2020

0260-8774/© 2020 Elsevier Ltd. All rights reserved.

water solubility so that they can be quickly adsorbed on the interface of the nanoemulsions and form continuous membranes around oil droplets, thus preventing aggregation between droplets. In addition, proteins can improve the bioavailability because they can inhibited the degradation of hydrophobic components that are susceptible to oxidation in gastrointestinal tract reaction (Lv et al., 2019; McClements et al., 2015).

In general, it is necessary to use high-energy input in preparation process in order to achieve better uniformity and stability. The ultrahigh pressure homogenization (UHPH) emulsifications technology can decompose into nano-droplets by generating strong turbulence and hydraulic shear stress (Zhang and Haque, 2015). Previous reference reported that the nanoemulsion was prepared by UHPH hand in soybean oil exhibited higher oxidative stability (Fernández-Ávila et al., 2015). The stability in UHPH-prepared nanoemulsions can be controlled by optimizing parameters such as homogenization conditions and type of protein emulsifiers (Lee and McClements, 2010).

Our previous study studied the chemical composition and antioxidant activity of extracts from SB (Zheng et al., 2017). The SBP extracts have also been added to bread to improve its nutritional value and shelf-life (Guo et al., 2019). Our present study is aimed (i) to use UHPH emulsifications technology to fabricate SBPO nanoemulsions, and explore the effects of different homogenization conditions on the stability; (ii) to determine whether the environmental conditions would have impact on the stability of different protein-stabilized SBPO nanoemulsions in order to select better emulsifier; (iii) to make an evaluation of CAA in vitro model. In summary, this study offers a reliable method for prepare excellent performance SBPO nanoemulsions delivery systems. And this study was delivering new idea for further extending the applications of SBPO as nutraceutical or functional dairy beverage.

2. Materials and methods

2.1. Materials and chemicals

The following SBPO were used: SBPO-G (Gansu, China), SBPO-X (Xinjiang, China), SBPO-H (Heilongjiang, China) and SBPO-Q (Qinghai, China). SBPO from different places of origin, which were gifted from factory, no antioxidants materials added in the production process. SC (S829595) from bovine milk and SPI (S832685) powder were purchased from Maclean Co. Ltd (Shanghai, China). According to the manufacturer, the composition of the SC was: 90% protein, 2% fat, 1% lactose, less than 6% ash and less than 12% moisture; and the composition of the SPI was: 90% protein, 3% fat, 4% ash and 7% moisture. WPI (Hilmar 9410) was purchased from Hilmar Food International, Inc. (Livingston, U.S.A). The composition of WPI was 93% protein, 1% fat, 4.7% ash and less than 6% moisture. Hexane, isopropanol, and other analytical chemicals or organic solvents, purchased from J&K Scientific Co. Ltd (Beijing, China).

2.2. Preparation of nanoemulsions

As shown in Fig. 1, 2.0% (w/v) concentration of SC, WPI, and SPI solutions were diluted in ultrapure water (18 MΩ cm at 25 °C). The SC, WPI, SPI and solutions were first heated at 140 °C, 85 °C, 95 °C and for 30 min in a closed centrifuge tube, respectively, for denaturing the disulfide and nonpolar bonds, leading to an increase in the emulsifying capacity (He et al., 2011). Then, the solutions were stirred and mixed for 4 h at 25 °C, and stored overnight at 4 °C after treatment in order to ensure complete hydration of the protein solution (Zhang and Haque, 2015; Xu et al., 2017). Next steps were determined according to the methods reported by reference and made some modifications (Yi et al., 2015). The SBPO (1:10, w/v) was added to the protein solutions and mixed (using SBPO-X to prepare nanoemulsions except for Section 2.8),

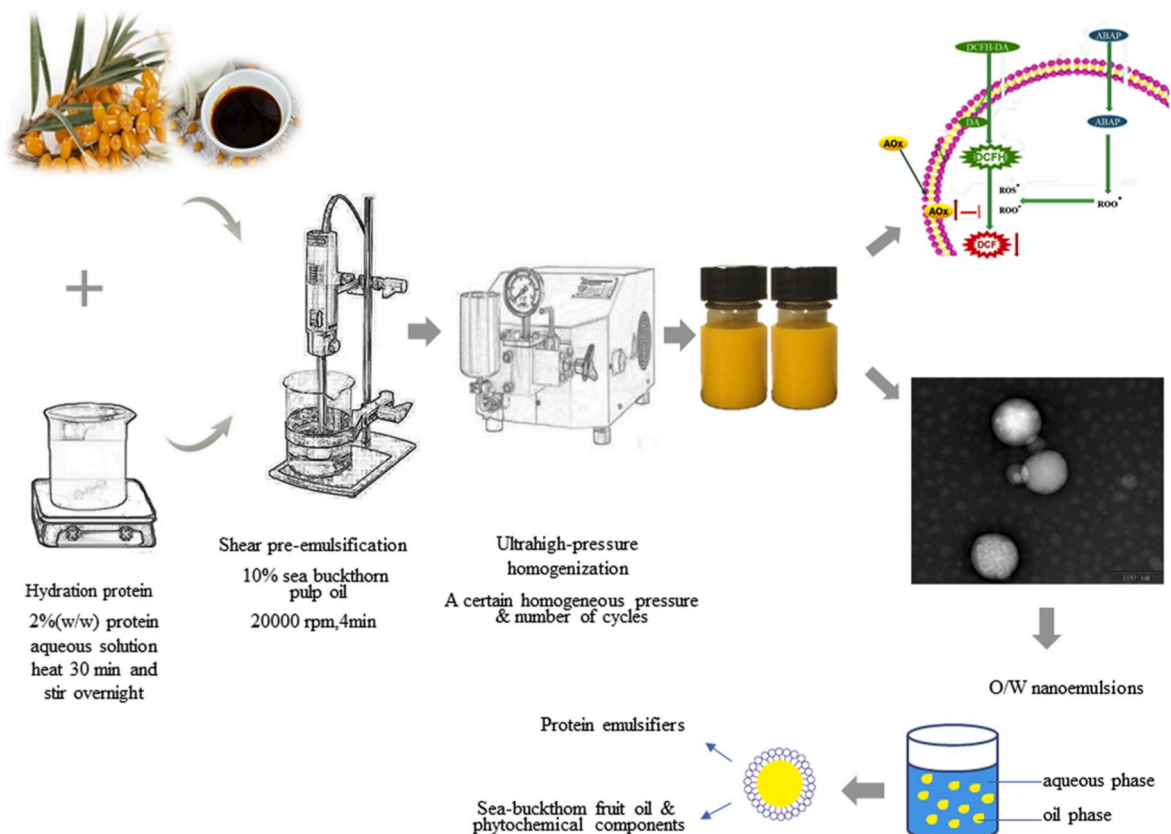


Fig. 1. Preparation process of protein-stabilized SBPO nanoemulsions.

which were sheared for 4 min at 20,000 rpm using a high-speed Ultra-Turrax blender (T25, IKA, Germany) to form crude emulsions. Then, the crude emulsions were further homogenized by high-pressure homogenizer (HPH 2000/4-SH5, GEA, Germany) using a two-stage homogenizing valve (the ratio of the first and second stage pressure was kept at 10 throughout). Using the above procedure, several samples were prepared by varying the homogenization pressure (first stage: 70–115 MPa) or cycles number (1–5) to study their effects on the properties of the nanoemulsions.

2.3. Determination of particle size and zeta potential

The mean particle size and zeta potential of the SBPO nanoparticles were determined using a Nano Brook Omni multi-angle particle sizer and High Sensitivity zeta-potential analyzer (Brookhaven Instruments, USA). The refractive indices of 1.33 for ultrapure water and 1.45 for the SBPO nanoparticles were applied. To improve the accuracy of measurements, the nanoemulsions were diluted 100 times before the measurements.

2.4. Physical stability

The method for measuring the physical stabilities of the SBPO nanoemulsions was decided according to the literature with slight modifications (Li et al., 2014; Xu et al., 2017). Three types of SBPO nanoemulsions diluted 100 times in ultrapure water were centrifuged at 2000×g for 20 min in a high-speed centrifuge. The sample of the supernatant in each SBPO nanoemulsions was withdrawn and mixed for 6 s. After that, the absorbance for each sample was detected at 500 nm wavelength. The Ke value is defined as the change of absorbance, which the emulsion was centrifuged at a certain speed for a period of time (He et al., 2011). The constant of centrifugal stability (Ke) was determined by the formula:

$$Ke = [(A - A_1)/A] \times 100\% \quad (1)$$

Where A and A_1 represent the absorbance values of the diluted SBPO nanoemulsions before and after centrifugation, respectively. According to Lambert-Beer law: $A = a \cdot b \cdot c$, the absorbance A is linearly related to the solution concentration when the thickness of the solution layer is b and the absorptivity a certain. Briefly, the effect of partition coefficient constant of Ke was the solution concentration c . The O/W nanoemulsions will produce delamination after centrifugation as above. Therefore, the stability of the emulsion can be accurately judged by the change of absorbance before and after centrifugation in actual measurements. Lower Ke values implied good physical stabilities of the SBPO nanoemulsions.

2.5. Morphology examination

TEM (JEM-1200EX, JEOL, and Tokyo, Japan) was applied to describe the morphologies of the three types of SBPO nanoparticles. The SBPO nanoemulsions with appropriate dilution were placed on a copper mesh and negatively stained for 5 min using phosphotungstic acid with a concentration of 2% (w/v). Finally, the copper mesh bearing SBPO nanoemulsions was observed and photographed under a transmission electron microscope at 200 kV.

2.6. Rheological characteristics measurements

The rheological characteristics of three protein-stabilized SBPO nanoemulsions were conducted by using a DHR-3 rheometer (DHR-3, Massachusetts, and U.S.A) with conical plate geometry. The diameter of plate was 40 mm and the distance between plates was 150 μ m. The viscosity was measured by increasing shear rates from 0.01 to 100 (1/s) at 25 °C. And the procedure of measurement was steady state flow mode.

The apparent viscosity data were plotted against the shear rate from the average measurements of 3 trials.

Next, about 1 mL of nanoemulsions was putted on the plate. The dynamic stress scanning mode was selected to determine the linear viscoelastic region of each sample. The shock shear pressure of sample was 1 Pa. The viscosity was measured by increasing angular frequency from 0.1 to 10 rad s⁻¹ at 25 °C. And the procedure of measurement was dynamic frequency scanning mode. The elastic modulus and viscous modulus data were plotted against the angular frequency from the mean measurements of 3 trials.

2.7. Effect of environmental conditions of nanoemulsions stability

Based on the results from section 3.1, for testing the effect of environmental conditions, nanoemulsions were prepared under the appropriate homogenization pressure (100, 100 and 115 MPa) and number of cycles (4, 4 and 5, respectively). The other steps were the same as Section 2.2.

2.7.1. Stability under different pH

The three SBPO nanoemulsions were diluted 100-fold in ultrapure water and adjusted to the desired pH (3, 5, 7, and 9) using 0.1 M HCl/NaOH.

2.7.2. Stability under different salinity

The SBPO nanoemulsions were diluted with different volumes of NaCl aqueous solution in order to prepare nanoemulsions with different NaCl concentrations (0, 50, 100, 150, and 200 mM).

2.7.3. Stability under different thermal treatment

The three types of SBPO nanoemulsions were placed in closed glass tubes incubated at 20, 40, 60, and 80 °C for half an hour. Using the above procedure, the samples were cooled at 25 °C. Subsequently, the characteristics (mean particle size, physical stability and zeta potential) of each sample were analyzed.

2.7.4. Determination of storage stability

The prepared sea-buckthorn oil nanoemulsions were pasteurized at 68 °C for 30 min, and then quickly cooled at 4 °C. Then, the storage stability was measured by detecting the mean particle sizes of the three protein-stabilized SBPO nanoemulsions after 0, 5, 10, 15, 20, 25, and 30 days of storage at 4 °C and 25 °C.

2.8. Determination of cellular antioxidant activity

According to the results of cell cytotoxicity, the antioxidant activity of SC-stabilized four different places of origin of SBPO nanoemulsions was evaluated at 100 μ g/mL treatment concentration. The method for culturing HepG₂ cells was decided according to the reports by Li et al. (2018) with minor modifications. HepG₂ cells were cultured at 10, 000/well on a 96-well microplate with a black bottom. The cells nutrient medium was prepared by DMEM–high glucose medium (25 mmol/L, 5 mL), which supplemented with 10% FBS and 1% streptomycin (75 μ g/mL) and penicillin (100 U/mL). Then, the cells were cultured in CO₂ incubator for one day (37 °C, 5% CO₂, 95% humidity). All liquid in well was then removed and each well was washed twice with PBS (1 mL, each time). After that, different concentrations of SC-stabilized SBFO nanoemulsions treatment solution of 100 μ L (containing 25 μ m DCFH-DA) was added to each well, and the cells were incubated for 1 h. All wells were washed twice with 100 μ L of PBS after removing growth medium. The PBS in the 96-well microplate was removed and 100 μ L of HBSS (including 600 μ m ABAP) was added immediately. Then, the 96-well microplate was placed on a Fluoroskan Ascent FL (ThermoScientific, USA) plate reader for reading. After that, the time-fluorescence value curve for each nanoemulsions sample was drew and integrated. The method for calculating cellular antioxidant activity (CAA) values was

decided according to reference with some slight modifications (Wolfe and Liu, 2008).

2.9. Statistical analysis

The results were expressed as mean ± standard deviation. All measurements were repeated at least 3 times. One-way ANOVA was used to analyze the differences between each group. Duncan's multi-range test

showed statistically significant differences in the mean values ($p < 0.05$). The data was statistically analyzed using the IBM SPSS Statistics 24.0. The data processing and charting are performed using Microsoft Excel 2013 and Origin 8.5.

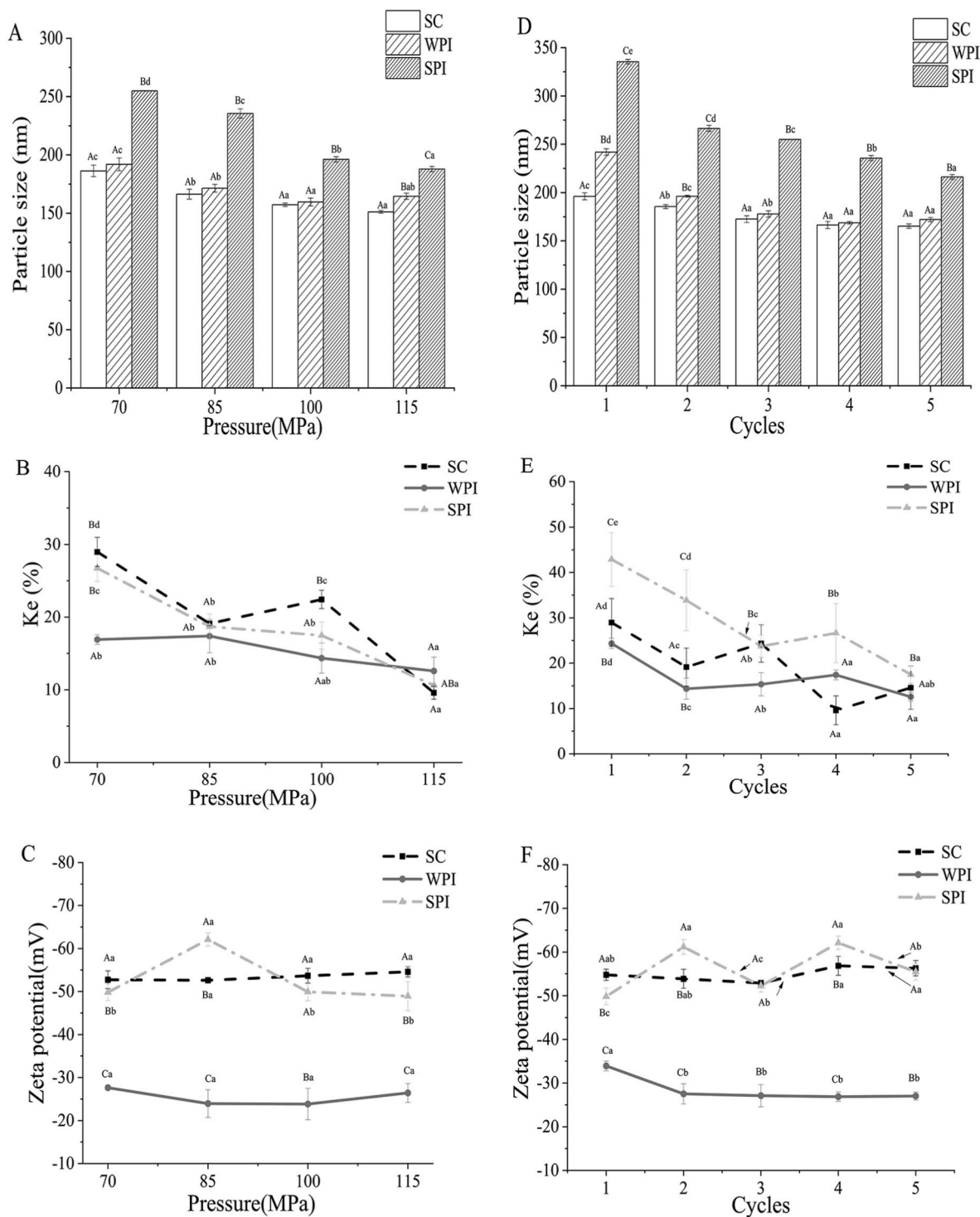


Fig. 2. Effects of homogenization pressure (A,B and C) and the number of cycles (D,E and F) on mean particle size, physical stability (Ke) and zeta potential of SC-, WPI- and SPI-stabilized SBPO nanoemulsions (Error bars: standard deviations of triplicate measurements). Different capital letters indicate significant differences ($p < 0.05$) between different protein nanoemulsions. Different lowercase letters indicate significant differences ($p < 0.05$) between same protein nanoemulsions.

3. Results and discussion

3.1. Effects of homogenization conditions on nanoemulsions properties

Fig. 2 shows the effects of homogenization conditions on the properties of SC-, WPI- and SPI-stabilized SBPO nanoemulsions such as mean particle size, physical stability and zeta potential were investigated.

The mean particle sizes of three protein-stabilized SBPO nanoemulsions were all ranged from 150 nm to 340 nm under UHPH treatments (Fig. 2A and B). Consequently, three different protein components could all form nanoemulsions. When the pressure was changed from 70 MPa to 100 MPa and the number of cycles changed from 1 to 4, a significant reduction in particle size of three protein-stabilized SBPO nanoemulsions was observed ($p < 0.05$). However, with a further increase in the pressure to 115 MPa and cycle time to 5, the particle size of the WPI-stabilized nanoemulsions began to increase. The possible reason was that the overtreatment effect of droplets at high energy input will increase surface area and interfacial tension, leading to the accumulation of the droplets particles and the formation of droplets in large-size emulsion formation (Wei et al., 2011). Contrary to the WPI-stabilized SBPO nanoemulsions, the mean particle size of SC- and SPI-stabilized nanoemulsions decreased with the increase of the pressure from 100 to 115 MPa and the increase of cycle number from 4 to 5. And the SC-stabilized SBPO nanoemulsions have the smallest particle size (151.19 nm). Taylor's formula demonstrates that higher pressures is corresponding to a higher shear rate and eventually produce small particle size (Mason et al., 2006; Li et al., 2014). On the other hand, the temperature of the nanoemulsions increased with the changes of different processing modes, which may lead to denaturation of the proteins (Riblett et al., 2001; Xu et al., 2017). It can be assumed that the denatured proteins cause the aggregation of the nanoparticles (Euston et al., 2002). But the denaturation temperature of SC and SPI is high, which close to 140 °C and 105 °C, respectively (Anema and Klostermeyer, 1997). When the pressure was 115 MPa and the cycle time was 5, the protein did not denature and the particle in this system was not aggregated.

The K_e value was inversely proportional with the physical stability of the emulsion sample. As shown in Fig. 2 (C and D), the K_e values of the three protein-stabilized SBPO nanoemulsions decreased with increasing homogenization pressure and cycle number, indicating the enhanced physical stability ($p < 0.05$). Tcholakova et al. (2005) also found that the surfactant absorb on the nanoparticle surface could enhance by an increase in pressure, which critically promoted the stability of the nanoemulsions.

Zeta potential of nanoemulsions is a measure of the intensity of mutual rejection or attraction between particles and particles. As shown in Fig. 2 (E and F), it was found that all the SBPO nanoemulsions were negatively charged under different homogenization conditions. The zeta potential of the WPI-stabilized nanoemulsions was approximately -25 mV, and that of SC- and SPI-stabilized nanoemulsions fluctuate around -55 mV. Tagne et al. (2008) indicated that higher absolute zeta potential correspond to greater nanoemulsions stability. Therefore, the SC- and SPI-stabilized SBPO nanoemulsions have relatively greater stability.

In summary, a smaller mean droplet size coupled with lower K_e values and higher zeta potential were achieved in the reconstituted sea buckthorn pulp oil nanoemulsions formed at relatively high homogenization conditions. The appropriate homogenization pressure of SC-, WPI- and SPI-stabilized SBPO nanoemulsions was 100 MPa, 100 MPa and 115 MPa, respectively. And the number of cycles was 4, 4 and 5, respectively.

3.2. Characterization

3.2.1. Basic characterization

Table 1 reports the basic characterization of the three SBPO nanoemulsions. The mean particle size of four different origin places of SBPO

Table 1

Basic characterization of the three types of SBPO nanoemulsions.

Compounds	Mean \pm SD (n = 3)		
	SC-stabilized SBPO	WPI-stabilized SBPO	SPI-stabilized SBPO
Mean particle size (nm)	160 \pm 1 ^a	160 \pm 3 ^a	188 \pm 2 ^b
K_e (%)	9.60 \pm 0.95 ^{ab}	12.57 \pm 1.19 ^a	10.62 \pm 0.37 ^b
Zeta potential (mV)	-54 \pm 2 ^a	-31 \pm 2 ^b	-49 \pm 3 ^a

Notes: means with different lower-case letter in the same row are significant different at $P < 0.05$.

nanoemulsions ranged from 160 to 188 nm, $K_e < 15\%$, and zeta potential ranged from -54 to -31 mV. The nanoemulsions system was uniform and stable. Fig. 3 shows a profile of particle size distribution in different protein-stabilized SBPO nanoemulsions, which has a slight effect. Intensity represents the relative strength of the measured intensity of droplets of different particle sizes in the nanoemulsions system (Lu et al., 2019). As shows in Fig. 3, the value of largest particle size is close to the mean particle size.

3.2.2. Morphology examination

Transmission electron microscope (TEM) observations provided positive images in which the nanoemulsions appeared as bright and spherical shapes with dark surroundings. The nanoemulsions are a water dispersing system and SBPO nanoemulsions droplets are dispersing materials, which exist in the form of monodisperse spheres. Previous research and patents used TEM imaging to obtain particle sizes based on scale (Manea et al., 2014). As shown in the micrographs (Fig. 4), UHPH reduced the mean particle size in SC-, WPI-stabilized SBPO nanoemulsions compared with SPI-stabilized SBPO nanoemulsions. In addition, the particle size of the three nanoemulsions was approximately 100 nm, which is significantly smaller than that measured by the nanometer particle size analyzer. There are two reasons for this discrepancy. Firstly, the treatment method is different. The multi-angle particle size and high-sensitivity zeta potential analyzer directly measures the emulsion system after dilution. The TEM pretreatment includes dilution, dropping onto copper mesh to dry, and then negative dyeing. The drying process may dehydrate the nanoemulsions and thus decrease its particle size. Secondly, the multi-angle particle sizer and high-sensitivity zeta potential analyzer detects the mean particle size under the normal distribution of the sample, while the TEM image

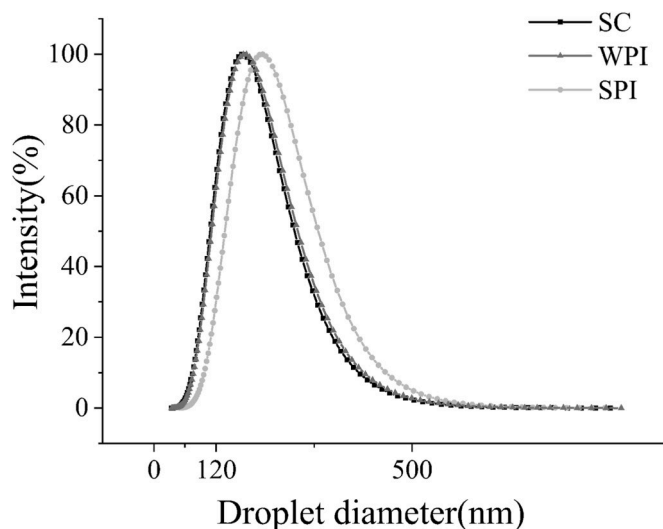


Fig. 3. Droplet size distribution of SC-, WPI- and SPI-stabilized SBPO nanoemulsions obtained using high homogenizing pressures.

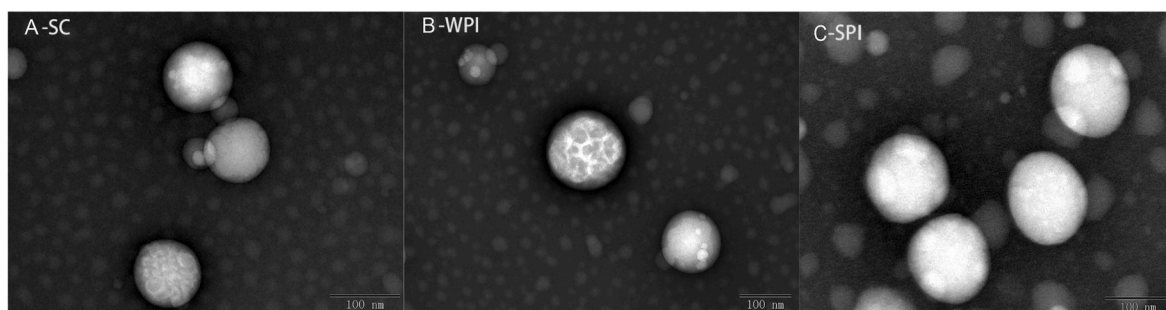


Fig. 4. Transmission electron microscopic image of SC-(A), WPI-(B) and SPI-stabilized(C) SBPO nanoemulsions (The scale bar for all images represents 100 nm).

obtains the droplet size within the field of view. These results confirmed that the droplets were nanoscale (<200 nm) and verified that the formulated emulsions were nanoemulsions.

3.2.3. Rheological characteristics

The rheological characteristics of nanoemulsions play an important role in delivery transport, processing and improving taste quality. In the food industry, some products need to have a lower viscosity to facilitate their transportation, packaging and drinking, such as beverages; others need to have a higher viscosity to make them taste better, such as dipping.

As shown in Fig. 5A, the apparent viscosities of three protein-stabilized SBPO nanoemulsions decreased with increasing shear rate. At a low shear rate of $<10 \text{ s}^{-1}$, the apparent viscosity declines significantly with an increase in shear rate, showing the characteristics of a shear thinning fluid, possibly because of the deformation and disintegration of flocs formed by droplets in the velocity field (Park et al., 2004). But with continuing increase in shear rate ($10 > \text{s}^{-1}$), the apparent viscosity remains unchanged, showing the characteristics of a Newtonian fluid. Either probably because all of the flocs are completely disrupted so that only individual droplets remain or because the rate of the floc formation and disintegration were equal, maintaining relative stability (Juliane et al., 2000). However, with the increase in shear rate, the viscosity of SPI-stabilized SBPO nanoemulsions increased significantly ($p < 0.05$). The reason probably because the SPI is composed by two globular protein fractions (glycinin and β -conglycinin). It is conjectured that the globular protein can be some extending and denaturation under the high temperatures and homogenization pressures (Desrumaux et al., 2000).

The ordinate in Fig. 5B represents the phase angle, $\tan \delta = G''/G'$, where G'' represents a viscous modulus and G' represents the elastic

modulus. The three types of SBPO nanoemulsions exhibit similar properties. When the angular frequency was $<1 \text{ rad/s}$, $\tan \delta > 1$ and the elastic modulus G' was smaller than the viscous modulus G'' , showing that the viscosity of the SBPO nanoemulsions was more obvious. When the angular frequency was $>1 \text{ rad/s}$, $\tan \delta < 1$ and the viscous modulus G'' was smaller than the elastic modulus G' , indicating that the elasticity of the SBPO nanoemulsions was more obvious.

3.3. Effect of environmental conditions on nanoemulsions stability

3.3.1. Stability under different pH

The surface charge plays important role in improving stability of nanoemulsions. The food proteins-stabilized nanoemulsions were different charged subject to pH variation because proteins are zwitterion (He et al., 2011). Fig. 6 shows the influence of pH on the SBPO nanoemulsions. As shown in Fig. 6 (A and B), the particle size and physical stability are slightly changed as the pH increased from 3 to 9, which indicates the nanoemulsions has a good homogeneity. However, an obvious jump occurred at pH 5. It can be seen that the different pH values have great influence on the K_e values, zeta potential and the stability of nanoemulsions.

At this point, the mean particle size of the SC, WPI, and SPI protein-stabilized SBPO nanoemulsions is approximately 240, 1200, and 1400 nm, respectively, and the corresponding K_e values of approximately 20%, 35%, and 48% are significantly higher than those at other pH levels ($p < 0.05$). This result could be explained by the isoelectric point theory. Harnsilawat et al. (2006) reported that when the pH approaches the isoelectric point of food proteins, electrostatic repulsion of the protein-stabilized SBPO nanoemulsions becomes significantly weak while the SBPO nanoparticles tend to be aggregated together through hydrophobic attractions and van der Waals interactions. For the above

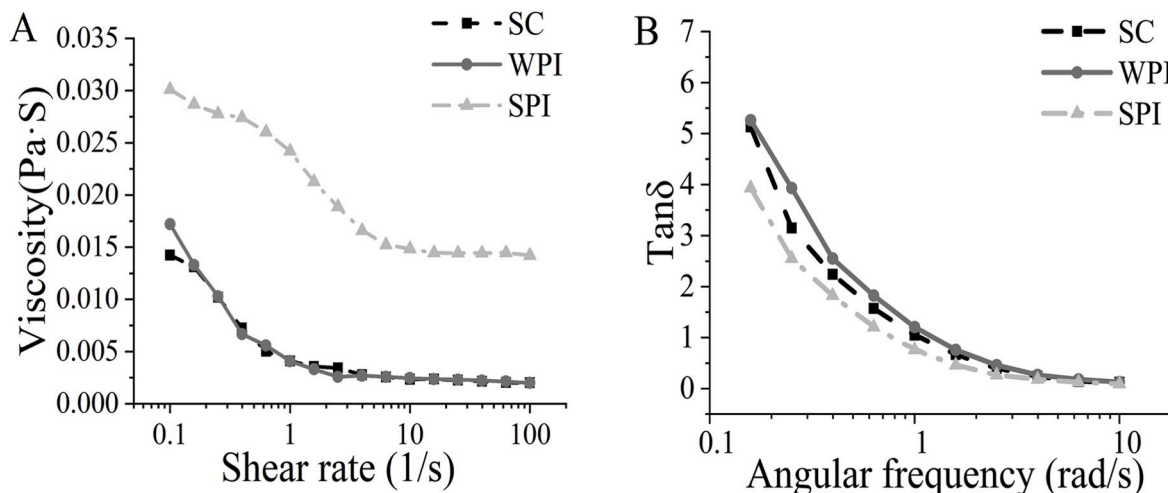


Fig. 5. Rheological characteristics of SC-, SPI- and WPI-stabilized SBPO nanoemulsions.

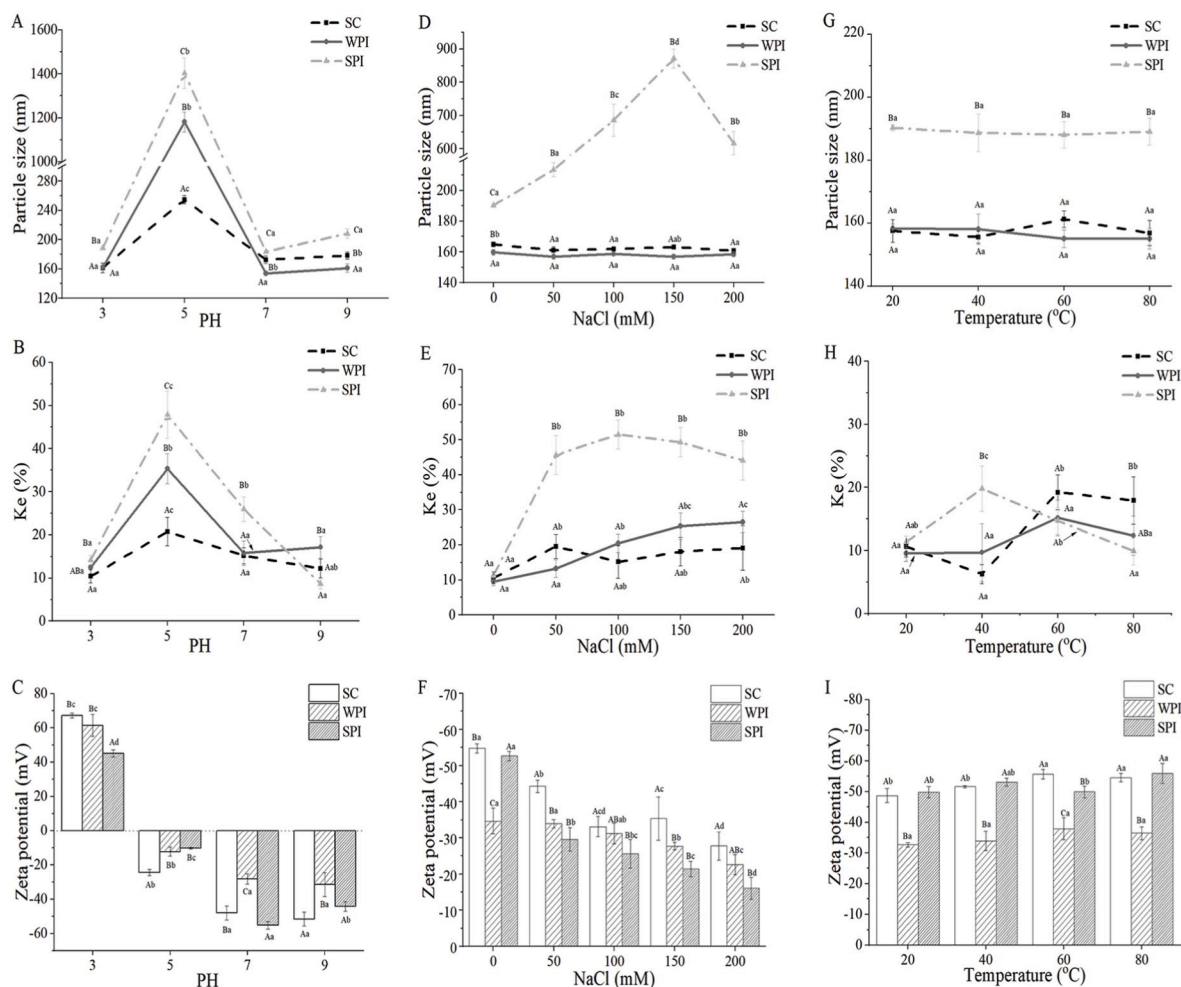


Fig. 6. Effects of pH (A, B and C), salinity (D, E and F) and temperature (G, H and I) on particle size, physical stability (K_e), and zeta potential of food protein stabilized nanoemulsions (Error bars: standard deviations of triplicate measurements). Different capital letters indicate significant differences ($p < 0.05$) between different protein nanoemulsions. Different lowercase letters indicate significant differences ($p < 0.05$) between same protein nanoemulsions.

three protein-stabilized SBPO nanoemulsions, they differ in molecular weight but isoelectric point all between 4 and 6 (Adachi et al., 2001; He et al., 2011; Permyakov and Berliner, 2000). And the zeta potentials of SC-, WPI- and SPI-stabilized SBPO nanoemulsions change from 67.1 to -51.6 mV, from 61.3 to -31.5 mV, and from 45.1 to -44.2 mV, respectively, with an increase in pH from 3 to 9. Previous studies have shown that higher absolute zeta potentials correspond to greater nanoemulsions stability. Because at larger zeta potentials, the charged droplets within nanoemulsions stronger repulsive interaction, which can overcome the natural tendency to aggregate (Tagne et al., 2008).

3.3.2. Stability under different salinity

A certain concentration of salt may be included in nanoemulsion-based delivery systems; therefore, the effects of ionic strength (0–200 mM NaCl) on the properties of SBPO nanoemulsions were examined (Fig. 6).

As shown in Fig. 6, the results show that the SC- and WPI- stabilized SBPO nanoemulsions are relatively stable in NaCl solutions, with slightly changes in particle size, the values of K_e and zeta potentials. It means that the two protein-stabilized SBPO nanoemulsions system have a stronger ability to resist the change of salt ion concentration. However, as for SPI-stabilized SBPO nanoemulsions, the mean particle size changed significantly from 190 to 872 nm under concentrations of 0–150 mM, respectively, as does K_e from 11.4% to 51.6% at concentrations of 0–100 mM ($p < 0.05$). The zeta potentials of the SPI-

stabilized SBPO nanoemulsions were also significantly influenced by increasing ionic strength, from -53.1 to -16.2 mV ($p < 0.05$). The salt ion can change the adsorption of protein at oil-water interface by changing the charge on the surface of protein emulsifier molecules, and affecting the emulsification. Also, the electrostatic repulsive force of oil-water interface will be reduced under the condition of high ionic strength, which will lead to flocculation and accumulation, and decrease of the stability of the system (Tippetts and Martini, 2012). The research of Zhai et al. (2011) also reported that the electrostatic repulsion of the oil-water interface can be reduced under the condition of high ionic strength, which leads to the flocculation and aggregation of the protein-stable emulsion. On the whole, the different protein-stabilized SBPO nanoemulsions stability of NaCl treatment with different concentrations in the system was in the order of: SC > WPI > SPI.

3.3.3. Stability under different thermal treatment

The delivery systems of nanoemulsions may be treated at different temperatures during processing, usage, and storage. It will affect the structure and physicochemical properties of protein emulsifier, and then affect the basic properties of nanoemulsions. We studied the change of the related properties of SBPO nanoemulsions in the range of 20–80 °C to explore the stability of the three protein-stabilized SBPO nanoemulsions at different temperatures. The results are shown in Fig. 6 (G, H and I).

It can be seen that there are no significant differences in the effect of

different temperature treatments on the mean particle size of three protein-stabilized SBPO nanoemulsions ($p > 0.05$). Lee et al. (2011) reported that WPI emulsified emulsion has better resistance to flocculation after heat treatment, which might be contained much higher active sulfhydryl concentrations. Emulsifiers with higher sulfhydryl could form the disulfide bonds in an O/W emulsion more efficiently, thus making the system more stable (Lee et al., 1992). However, the mean particle size of the SPI-stabilized SBPO nanoemulsions was obviously different from the other two kinds. Tokle et al. (2011) show that when the emulsion temperature increases, the adsorbed globular protein produces thermal denaturation and nonpolar groups are exposed which promoted the content of hydrophobic groups, thus the particle of SBPO nanoemulsions is more likely flocculation and aggregation. These differences of structural might be sufficient to subtly affect the properties of the emulsion Like we mentioned in Section 3.2.3, SPI had two globular protein fractions, which may explain why SPI-stabilized SBPO nanoemulsions was prone to form larger droplets. As a whole, all the nanoemulsions were relatively stable to droplet aggregation and creaming after heat treatments with little changes in mean particle size.

The range of Ke of the three kinds SBPO (SC, WPI, SPI) nanoemulsions was 6.3%–19.2%, 9.5%–15.2% and 10.3%–19.7%, respectively. The minimum values of Ke were obtained at 40 °C, 20 °C and 80 °C, respectively, and the centrifugal stability was the strongest at the corresponding temperature. The range of zeta potentials of SC-, WPI-, SPI-stabilized nanoemulsions was $-48.7 \sim -55.7$ mV, $-32.6 \sim -37.8$ mV and $-49.83 \sim -55.92$ mV, respectively. The absolute value of zeta potentials shows increasing trends with the temperature from 20 to 80 °C.

The three types of SBPO nanoemulsions have reasonable temperature stability at different temperatures ranging from 20 to 80 °C. Previous studies indicated that heat treatment can enhance the stability of protein-stabilized nanoemulsions against aggregation, by denaturing the disulfide and nonpolar bonds and increasing the emulsifying capacity (Xu et al., 2017). To summarize, the order of the three protein-stabilized SBPO nanoemulsions stability of different temperature in the system was: SC > WPI > SPI.

3.3.4. Storage stability

As shown in Fig. 7, the SC-stabilized SBPO nanoemulsions all showed fairly good stability over 30 days at 4 °C and 25 °C, with slightly differences in droplet size. But the mean particle size of SPI- and WPI-stabilized SBPO nanoemulsions stored at 4 °C for 30 days was increased significantly, with a range of 159.7–202.6 nm and 186.7–256.9 nm, respectively. However, more drastic changes in

particle size of storage at 25 °C for 30 days in this study can be observed with a range of 186.7–267.1 nm (SPI) and 186.7–222.7 nm (WPI), respectively.

The differences in storage stability of different protein-stabilized SBPO nanoemulsions could be due to the thermodynamic stability and kinetic stability of its embedded structure. The small probability of interdroplet collision during storage at 4 °C prevents any increase in droplet size. The smaller droplets are more stable against gravity separation, and aggregation of the SBPO nanoparticles would be less likely. However, the Brownian movement between particles intensifies and the collision probability increases at higher storage temperatures, which resulting in droplet agglomeration. This phenomenon is more pronounced in emulsions with larger particle size. Fernández-Ávila et al. (2015) found that nanoemulsions prepared by ultrahigh-pressure homogenization had better stability than those prepared by conventional homogenization.

3.4. Cellular antioxidant activity of SC-stabilized SBPO nanoemulsions

The above results prove that SC as emulsifier stable SBPO nanoemulsions show excellent physical stability under different conditions and the best storage stability. In this section, four different places of origin (SBPO-G, SBPO-X, SBPO-H, and SBPO-Q) of SBPO were prepared with SC as emulsifier to make an evaluation of CAA in vitro biological model. As shown in Table 2 the mean particle size of four different places of origin of SBPO nanoemulsions ranged from 156.3 to 173.4 nm, zeta potential ranged from -50.51 to 57.95 mV, and $Ke < 15\%$. The SC-stabilized SBPO nanoemulsions system was uniform and stable.

The antioxidant activity of four different places of origin of SC-stabilized SBPO nanoemulsions were quantitatively analyzed by the previously established standard curve of quercetin. As shown in Fig. 8, the CAA unit of these four different origins places SBPO nanoemulsions

Table 2

Basic properties of four different places of origin SC-stabilized SBPO nanoemulsions.

Compounds	Mean \pm SD (n = 3)			
	1	2	3	4
Particle size (nm)	173.4 \pm 6.86 ^a	160.5 \pm 7.00 ^b	169.3 \pm 8.68 ^a	156.3 \pm 6.31 ^b
Ke (%)	14.32 \pm 2.12 ^a	9.59 \pm 1.18 ^b	14.58 \pm 1.76 ^a	11.34 \pm 0.54 ^b
Zeta potential (mV)	-50.51 \pm 4.43 ^a	-56.95 \pm 3.58 ^a	-55.18 \pm 1.28 ^a	-57.95 \pm 1.55 ^a

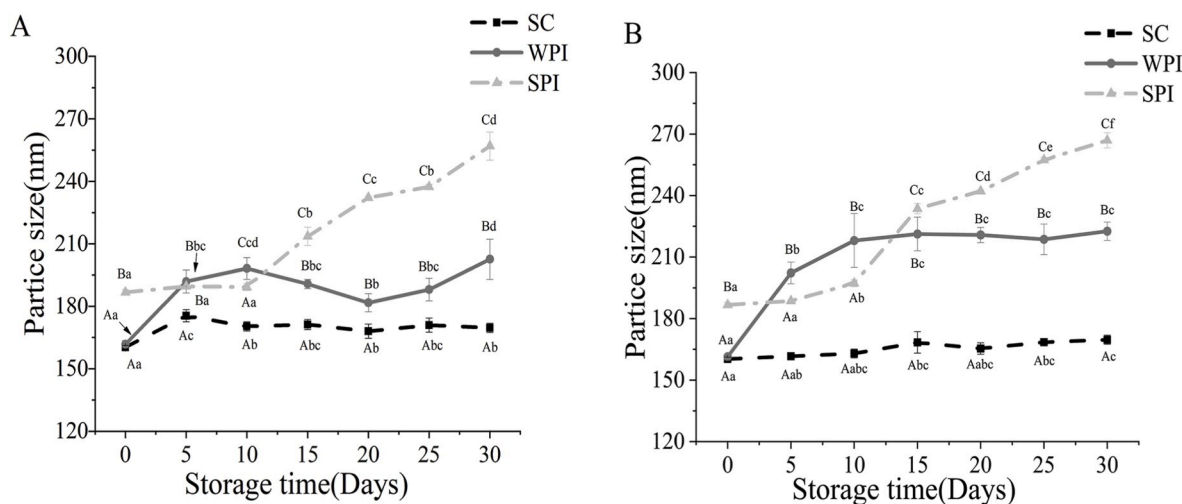


Fig. 7. Storage stability of food protein-stabilized nanoemulsions at 4 °C (A) and 25 °C (B). Different capital letters indicate significant differences ($p < 0.05$) between different protein nanoemulsions. Different lowercase letters indicate significant differences ($p < 0.05$) between same protein nanoemulsions.

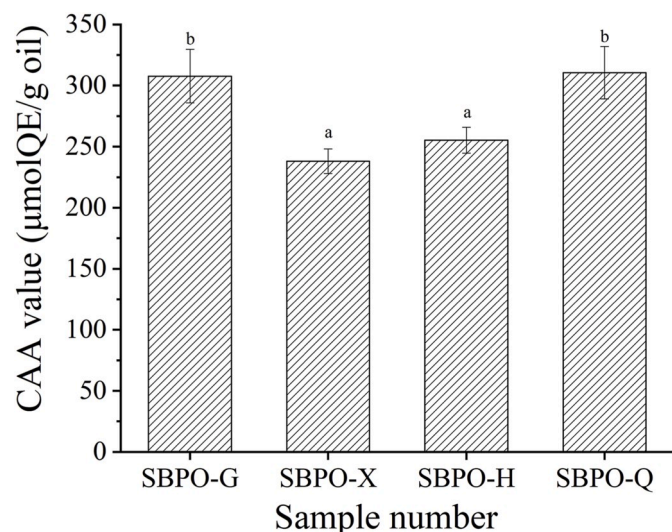


Fig. 8. Cellular antioxidant activity of SC-stabilized SBPO nanoemulsions. (Error bars: standard deviations of triplicate measurements).

from high to low were 310.54 ± 21.48 µmol of QE/g oil (SBPO-Q) > 307.71 ± 21.86 µmol of QE/g oil (SBPO-G) > 255.24 ± 10.55 µmol of QE/g oil (SBPO-H) > 238.03 ± 10.09 µmol of QE/g oil (SBPO-X). These results indicated that SC-stabilized SBPO nanoemulsions all showed good cellular antioxidant, which can effectively protect the active substances in SBPO. SBPO-G and SBPO-Q nanoemulsions exhibited significantly higher CAA than other nanoemulsions.

The reason may be related to the difference of SBPO nanoemulsions chemicals composition from different places of origin (Table 3 and 4). Our previous researches have shown that when there was no significantly difference in the fatty acid composition of SBPO, the antioxidant activity of the SBPO was related to the content of the lipids phytochemical, especially phenols compounds (Zheng et al., 2017). And the similar results were observed in CAA biological model (Liu et al., 2019). Although minor constituents of oil are often used to represent the antioxidant activity of oils, our recent research suggests that the oil itself, such as the type and saturation of triglycerides may affect the overall results (Lu et al., 2019). Fatty acids with different chain lengths or degree of saturation could alter the cell membrane morphology and fluidity, fatty acids transporter and related gene expression, which cause the difference in uptake and bioavailability of antioxidant components into cells (Yan et al., 2019). In addition, oils with similar fatty acid composition had different CAA due to the content of the minor lipids phytochemical. For example, some lipids phytochemical like phenols compounds has special functional groups, which can combine with free radicals by releasing active hydrogen on the hydroxyl group (Gulcin et al., 2020). In short, the results of the CAA were due to the combined effects of triglycerides and lipids phytochemical of the oil and the detail information remain to be further revealed.

CAA evaluation model was initially applied to antioxidant substances or food extracts (Chen et al., 2018). However, it is feasible to apply this method to a range of complex edible natural products including liposomes and O/W nanoemulsions (Liang et al., 2017; Lu et al., 2019), which is a good trial for the CAA assay.

4. Conclusions

In summary, food protein-stabilized nanoemulsions were successfully produced. The effects of different processing modes, environmental conditions and storage on the properties including mean particle size, zeta potential and physical stability of the SBPO nanoemulsions were explored. The results shown in SC-stabilized SBPO nanoemulsions exhibited relatively good stability against pH, salinity, high

Table 3

Mean ± SD values of fatty acid composition of four different places of origin SBPO samples (%).

Compounds	Mean ± SD (n = 3)			
	SBPO-G	SBPO-X	SBPO-H	SBPO-Q
C14:0	0.61 ± 0.02 ^c	0.18 ± 0.01 ^a	0.58 ± 0.01 ^c	0.46 ± 0.01 ^b
C16:0	28.9 ± 0.3 ^a	32.5 ± 0.2 ^c	31.0 ± 0.1 ^b	31.2 ± 0.2 ^b
C16:1	34.4 ± 0.6 ^{ab}	32.2 ± 0.1 ^a	33.9 ± 0.2 ^{ab}	35.2 ± 0.2 ^b
C18:0	2.77 ± 0.01 ^d	2.36 ± 0.02 ^c	1.53 ± 0.01 ^a	1.99 ± 0.02 ^b
C18:1	21.7 ± 0.5 ^{ab}	22.9 ± 0.3 ^b	21.0 ± 0.1 ^{ab}	20.3 ± 0.5 ^a
C18:2	8.19 ± 0.15 ^b	7.21 ± 0.05 ^a	8.01 ± 0.12 ^b	7.16 ± 0.04 ^a
C18:3	3.05 ± 0.01 ^c	2.52 ± 0.03 ^a	2.88 ± 0.02 ^b	3.03 ± 0.02 ^c

Notes: means with different lower-case letter in the same row are significant different at $p < 0.05$.

Table 4

Mean ± SD values of lipids phytochemical of four different places of origin SBPO samples (mg/kg).

Compounds	Mean ± SD (n = 3)			
	SBPO-G	SBPO-X	SBPO-H	SBPO-Q
Tocopherols (mg/kg)				
α-tocopherol	213 ± 3 ^a	202 ± 3 ^a	200 ± 3 ^a	208 ± 1 ^a
β-tocopherol	11.0 ± 0.1 ^{bc}	9.9 ± 0.5 ^b	7.0 ± 0.1 ^a	11.6 ± 0.1 ^c
γ-tocopherol	12.3 ± 0.1 ^d	2.3 ± 0.2 ^a	5.6 ± 0.2 ^b	9.2 ± 0.1 ^c
δ-tocopherol	5.3 ± 0.3 ^a	14.3 ± 0.4 ^b	6.2 ± 0.5 ^a	15.2 ± 0.2 ^b
Phytosterols (mg/kg)				
β-sitosterol	8074 ± 9 ^b	7178 ± 51 ^a	10,736 ± 87 ^c	8011 ± 23 ^b
stigmasterol	327 ± 6 ^b	503 ± 10 ^c	104 ± 7 ^a	109 ± 4 ^a
campesterol	150 ± 8 ^b	77 ± 12 ^a	251 ± 2 ^c	345 ± 12 ^d
β-carotene (mg/kg)	223 ± 6 ^a	204 ± 7 ^a	226 ± 3 ^a	241 ± 10 ^a

Notes: means with different lower-case letter in the same row are significant different at $P < 0.05$.

temperature, and storage periods. Further, in the vitro CAA model, SC-stabilized SBPO nanoemulsions prepared by optimized homogenization conditions and wall materials showed good antioxidant activity. These results indicated that SC-stabilized nanoemulsions are a promising carrier for nutraceutical, which can effectively protect the active substances in SBPO. This study provides a new idea for further extending the applications of SBPO as nutraceutical or functional dairy beverage.

Declaration of competing interest

The authors declared that they have no conflicts of interest to this work. We declare that we do not have any commercial or associative interest that represents a conflict of interest in connection with the work submitted.

CRediT authorship contribution statement

Ming Chang: Writing - original draft. **Yiwen Guo:** Writing - review & editing. **Zhongrong Jiang:** Formal analysis. **Longkai Shi:** Software. **Tao Zhang:** Methodology. **Yandan Wang:** Supervision. **Mengyue Gong:** Validation. **Tao Wang:** Visualization. **Ruixue Lin:** Investigation. **Ruijie Liu:** Writing - review & editing. **Yong Wang:** Data curation. **Qingzhe Jin:** Conceptualization. **Xingguo Wang:** Funding acquisition.

Acknowledgements

This work was supported by the National Natural Science Foundation of China (Grant No. 31872895), the national first-class discipline program of Food Science and Technology (JUFSTR20180202).

References

- Adachi, M., Takenaka, Y., Gidamis, A.B., Mikami, B., Utsumi, S., 2001. Crystal structure of soybean proglycinin alab1b homotrimer. *J. Mol. Biol.* 305 (2), 291–305. <https://doi.org/10.1006/jmbi.2000.4310>.
- Anema, S.G., Klostermeyer, H., 1997. Heat-induced, pH-dependent dissociation of casein micelles on heating reconstituted skim milk at temperatures below 100 °C. *J. Agric. Food Chem.* 45 (4), 1108–1115.
- Chen, C., Wang, L., Wang, R., Luo, X.H., Li, Y.F., Li, J., Li, Y.N., Chen, Z.X., 2018. Phenolic contents, cellular antioxidant activity and antiproliferative capacity of different varieties of oats. *Food Chem.* 239, 260–267. <https://doi.org/10.1016/j.foodchem.2017.06.104>.
- Desrumaux, A., Loisel, C., Marcand, J., 2000. Performances of a new high pressure homogenizer to make fine food emulsions. ICEF8, International Congress on Engineering and Food, Puebla (Mexico), 9–13 April, 2000.
- Euston, S.R., Finnigan, S.R., Hirst, R.L., 2002. Kinetics of droplet aggregation in heated whey protein-stabilized emulsions: effect of polysaccharides. *Food Hydrocolloids* 16 (5), 499–505. [https://doi.org/10.1016/S0268-005X\(01\)00130-8](https://doi.org/10.1016/S0268-005X(01)00130-8).
- Fatima, T., Snyder, C.L., Schroeder, W.R., Cram, D., Datla, R., Wishart, D., Weselake, R. J., Krishna, P., 2012. Fatty acid composition of developing sea buckthorn (*Hippophae rhamnoides* L.) berry and the transcriptome of the mature seed. *PLoS One* 7 (4), e34099. <https://doi.org/10.1371/journal.pone.0034099>.
- Fernández-Ávila, C., Escriu, R., Trujillo, A.J., 2015. Ultra-High Pressure Homogenization enhances physicochemical properties of soy protein isolate-stabilized emulsions. *Food Res. Int.* 75, 357–366. <https://doi.org/10.1016/j.foodchem.2016.04.019>.
- Gao, S., Guo, Q., Qin, C.G., Shang, R., Zhang, Z.S., 2017. sea buckthorn fruit oil extract alleviates insulin resistance through the PI3K/akt signaling pathway in type 2 diabetes mellitus cells and rats. *J. Agric. Food Chem.* 65 (7), 1328–1336. <https://doi.org/10.1021/acs.jafc.6b04682>.
- George, S. D. St, Cenkowski, S., 2007. Influence of harvest time on the quality of oil-based compounds in sea buckthorn (*Hippophae rhamnoides* L. ssp. *sinensis*) seed and fruit. *J. Agric. Food Chem.* 55 (20), 8054–8061. <https://doi.org/10.1021/jf070772f>.
- Gulcin, İ., 2020. Antioxidants and antioxidant methods: an updated overview. *Arch. Toxicol.* 94, 651–715. <https://doi.org/10.1007/s00204-020-02689-3>.
- Guo, X., Shi, L.K., Yang, S., Yang, R.J., Dai, X.Y., Zhang, T., Liu, R.J., Chang, M., Jin, Q.Z., Wang, X.G., 2019. Effect of sea-buckthorn pulp and flaxseed residues on quality and shelf life of bread. *Food Funct.* 10 (7). <https://doi.org/10.1039/C8FO02511H>.
- Harnsilawat, T., Pongsawatmanit, R., McClements, D.J., 2006. Characterization of β -lactoglobulin-sodium alginate interactions in aqueous solutions: a calorimetry, light scattering, electrophoretic mobility and solubility study. *Food Hydrocolloids* 20 (5), 577–585. <https://doi.org/10.1016/j.foodhyd.2005.05.005>.
- He, W., Tan, Y., Tian, Z., Chen, L., Hu, F., Wu, W., 2011. Food protein-stabilized nanoemulsions as potential delivery systems for poorly water-soluble drugs: preparation, in vitro characterization, and pharmacokinetics in rats. *Int. J. Nanomed.* 6 (6), 521–533. <https://doi.org/10.1021/nn100307j>.
- Juliane, F., Anne, D., Jérémie, L., 2000. Effect of high-pressure homogenization on droplet size distributions and rheological properties of model oil-in-water emulsions. *Innov Food Sci Emerg* 1 (2), 127–134. [https://doi.org/10.1016/S1466-8564\(00\)00012-6](https://doi.org/10.1016/S1466-8564(00)00012-6).
- Joye, I.J., Davidov-Pardo, G., McClements, D.J., 2014. Nanotechnology for increased micronutrient bioavailability. *Trends Food Sci. Technol.* 40 (2), 168–182. <https://doi.org/10.1016/j.tifs.2014.08.006>.
- Lee, S.J., Choi, S.J., Li, Y., Decker, E.A., McClements, D.J., 2011. Protein-stabilized nanoemulsions and emulsions: comparison of physicochemical stability, lipid oxidation, and lipase digestibility. *J. Agric. Food Chem.* 59 (1), 415–427. <https://doi.org/10.1021/jf103511v>.
- Lee, S.J., McClements, D.J., 2010. Fabrication of protein-stabilized nanoemulsions using a combined homogenization and amphiphilic solvent dissolution/evaporation approach. *Food Hydrocolloids* 24 (6–7), 560–569. <https://doi.org/10.1016/j.foodhyd.2010.02.002>.
- Lee, S.Y., Morr, C.V., Ha, E.Y.W., 1992. Structural and functional properties of caseinate and whey protein isolate as affected by temperature and pH. *J. Food Sci.* 57 (5), 1210–1229.
- Lu, M.Y., Zhang, T., Jiang, Z.R., Guo, Y.W., Qiu, F.C., Liu, R.R., Zhang, L.S., Chang, M., Liu, R.J., Jin, Q.Z., Wang, X.G., 2019. LWT - Food Sci. Technol. (Lebensmittel-Wissenschaft -Technol.) 108948. <https://doi.org/10.1016/j.lwt.2019.108948>.
- Lv, S.S., Zhang, Y.H., Tan, H.Y., Zhang, R.J., McClements, D.J., 2019. Vitamin E encapsulation within oil-in-water emulsions: impact of emulsifier type on physicochemical stability and bioaccessibility. *J. Agric. Food Chem.* 67 (5), 1521–1529. <https://doi.org/10.1021/acs.jafc.8b06347>.
- Liang, T.S., Guan, R.F., Wang, Z., Shen, H.T., Xia, Q.L., Liu, M.Q., 2017. Comparison of anticancer activity and antioxidant activity between cyanidin-3-O-glucoside liposomes and cyanidin-3-O-glucoside in Caco-2 cells in vitro. *RSC Adv.* 7 (59), 37359–37368. <https://doi.org/10.1039/C7RA06387C>.
- Li, M., Ma, Y., Cui, J., 2014. Whey-protein-stabilized nanoemulsions as a potential delivery system for water-insoluble curcumin. *LWT - Food Sci. Technol. (Lebensmittel-Wissenschaft -Technol.)* 59 (1), 49–58. <https://doi.org/10.1016/j.lwt.2014.04.054>.
- Li, X.J., Shen, Y.B., Wu, G.C., Qi, X.G., Zhang, H., Wang, L., Qian, H.F., 2018. Determination of key active components in different edible oils affecting lipid accumulation and reactive oxygen species production in HepG2 cells. *J. Agric. Food Chem.* 66 (45), 11943–11956. <https://doi.org/10.1021/acs.jafc.8b04563>.
- Liu, R.J., Lu, M.Y., Zhang, T., Zahng, Z.Y., Jin, Q.Z., Chang, M., Wang, X.G., 2019. Evaluation of the antioxidant properties of micronutrients in different vegetable oils. *Eur. J. Lipid Sci. Technol.* <https://doi.org/10.1002/ejlt.201900079>.
- Manea, A.M., Ungureanu, C., Meghea, A., 2014. Effect of vegetable oils on obtaining lipid nanocarriers for sea buckthorn extract encapsulation. *Comptes rendus - Chim* 17 (9), 934–943. <https://doi.org/10.1016/j.crci.2013.10.020>.
- Mason, T.G., Wilking, J.N., Meleson, K., Chang, C.B., Graves, S.M., 2006. Nanoemulsions: formation, structure, and physical properties. *J Phys-Condens Mat* 18 (41), R635. <https://doi.org/10.1088/0953-8984/18/41/R01>.
- McClements, D.J., Zou, L., Zhang, R., Trujillo, L.S., Taha Kumosani, T., Xiao, H., 2015. Enhancing nutraceutical performance using excipient foods: designing food structures and compositions to increase bioavailability. *Compre Rev Food* 14 (6), 824–847. <https://doi.org/10.1111/1541-4337.12170>, 2015.
- Park, S., Chung, M.G., Yoo, B., 2004. Effect of octenylsuccinylation on rheological properties of corn starch pastes. *Starch* 56 (9), 399–406. <https://doi.org/10.1002/star.200300274>.
- Permyakov, E.A., Berliner, L.J., 2000. alpha-Lactalbumin: structure and function. *FEBS (Fed. Eur. Biochem. Soc.) Lett.* 473 (3), 269–274. [https://doi.org/10.1016/S0014-5793\(00\)01546-5](https://doi.org/10.1016/S0014-5793(00)01546-5).
- Rave, M.C., Echeverri, J.D., Salamanca, C.H., 2020. Improvement of the physical stability of oil-in-water nanoemulsions elaborated with Sacha inchi oil employing ultra-high-pressure homogenization. *J. Food Eng.* 273, 109801, 1016/j.jfoodeng.2019.109801.
- Riblett, A.L., Herald, T.J., Schmidt, K.A., Tilley, K.A., 2001. Characterization of beta-conglycinin and glycinin soy protein fractions from four selected soybean genotypes. *J. Agric. Food Chem.* 49 (10), 4983–4989. <https://doi.org/10.1021/jf0105081>.
- Singh, H., Sarkar, A., 2011. Behaviour of protein-stabilised emulsions under various physiological conditions. *Adv Colloid Interfac* 165 (1), 47–57. <https://doi.org/10.1016/j.cis.2011.02.001>.
- Tagne, J.B., Kakumanu, S., Nicolosi, R.J., 2008. Nanoemulsion preparations of the anticancer drug dacarbazine significantly increase its efficacy in a xenograft mouse melanoma model. *Mol. Pharm.* 5 (6), 1055–1063. <https://doi.org/10.1021/mp8000556>.
- Tippetts, M., Martini, S., 2012. Influence of L-carrageenan, pectin, and gelatin on the physicochemical properties and stability of milk protein-stabilized emulsions. *J. Food Sci.* 77 (2), C253–C260. <https://doi.org/10.1111/j.1750-3841.2011.02576.x>.
- Tokle, T., McClements, D.J., 2011. Physicochemical properties of lactoferrin stabilized oil-in-water emulsions: effects of pH, salt and heating. *Food Hydrocolloids* 25 (5), 976–982. <https://doi.org/10.1016/j.foodhyd.2010.09.012>.
- Wei, H., Tan, Y., Tian, Z., Chen, L., Hu, F., Wei, W., 2011. Food protein-stabilized nanoemulsions as potential delivery systems for poorly water-soluble drugs: preparation, in vitro characterization, and pharmacokinetics in rats. *Int. J. Nanomed.* 6 (6), 521–533. <https://doi.org/10.2147/IJN.S17282>.
- Wolfe, K.L., Liu, R.H., 2008. Structure-activity relationships of flavonoids in the cellular antioxidant activity assay. *J. Agric. Food Chem.* 56 (18), 8404–8411. <https://doi.org/10.1021/jf8013074>.
- Xu, J., Mukherjee, D., Chang, S.K.C., 2017. Physicochemical properties and storage stability of soybean protein nanoemulsions prepared by ultra-high pressure homogenization. *Food Chem.* 240, 1005–1013. <https://doi.org/10.1016/j.foodchem.2017.07.077>.
- Yan, Q.X., Tang, S.X., Zhou, C.S., Han, X.F., Tang, Z.L., 2019. Effects of free fatty acids with different chain lengths and degrees of saturability on the milk fat synthesis in primary cultured bovine mammary epithelial cells. *J. Agric. Food Chem.* 67 (31), 8485–8492. <https://doi.org/10.1021/acs.jafc.9b02905>.
- Yi, J., Lam, T.I., Yokoyama, W., Cheng, L.W., Zhong, F., 2015. Beta-carotene encapsulated in food protein nanoparticles reduces peroxy radical oxidation in Caco-2 cells. *Food Hydrocolloids* 43, 31–40.
- Zhai, Z.J., Wooster, T.J., Hoffmann, S.V., Lee, T.H., Augustin, M.A., Aguilar, M.I., 2011. Structural rearrangement of β -lactoglobulin at different oil-water interfaces and its effect on emulsion stability. *Langmuir* 27 (15), 9227–9236. <https://doi.org/10.1021/la201483y>.
- Zhang, X., Haque, Z.Z., 2015. Generation and stabilization of whey based monodisperse nanoemulsions using ultra-high pressure homogenization and small amphiphilic co-emulsifier combinations. *J. Agric. Food Chem.* 63 (45), 10070–10077. <https://doi.org/10.1021/acs.jafc.5b03889>.
- Zheng, L., Shi, L.K., Zhao, C.W., Jin, Q.Z., Wang, X.G., 2017. Fatty acid, phytochemical, oxidative stability and in vitro antioxidant property of sea buckthorn (*Hippophae rhamnoides* L.) oils extracted by supercritical and subcritical technologies. *LWT - Food Sci. Technol. (Lebensmittel-Wissenschaft -Technol.)* 86, 507–513. <https://doi.org/10.1016/j.lwt.2017.08.042>.
- Zielińska, A., Nowak, I., 2017. Abundance of active ingredients in sea-buckthorn oil. *Lipids Health Dis.* 16 (1), 95–105. <https://doi.org/10.1186/s12944-017-0469-7>.